OPEN ACCESS
Journal of Innovative Optical Health Sciences
Vol. 14, No. 1 (2021) 2140006 (9 pages)

DOI: 10.1142/S179354582140006X

World Scientific
www.worldscientific.com

Monitoring of edema progression in permanent and transient MCAO model using SS-OCT

Yao Yu*, Ziyue Meng*, Ang Li*, Yang Lin*, Jian Liu*, Yushu Ma†,
Yi Wang* and Zhenhe Ma*,‡
*School of Control Engineering
Northeastern University at Qinhuangdao
Qinhuangdao 066004, P. R. China

†School of Computer Science and Engineering
Northeastern University
Shenyang 110169, P. R. China
‡mazhenhe@163.com

Received 21 September 2020
Accepted 2 December 2020
Published 4 January 2021

Cerebral edema is a severe complication of acute ischemic stroke with high mortality but limited treatment. Although parameters such as brain water content and intracranial pressure may represent the global assessment of edema, optical properties can appear heterogeneously throughout the cerebral tissue relative to the site of injury. In this study, we have monitored the edema formation and progression in both permanent and transient middle cerebral artery occlusion models in rats. Edema was reflected by the decrease of optical attenuation coefficient (OAC) value in OCT system. By utilizing swept-source optical coherence tomography (SS-OCT), we found that in photochemically induced permanent focal stroke model, both the edema size and edema index, steadily developed until the end of monitor (7 h). Comparatively, when transient ischemia was introduced with endothelin-1 (ET-1), the edema was detected as early as 15 min, and began to recover after 30 min until monitor was finished (3 h). Despite the majority of the edema being recovered to some extent, the condition of a small region within the edema kept deteriorating, presumably due to the reperfusion damage which might result in serious clinical outcomes. Our study has compared the edema characteristics from two different acute ischemic stroke situations. This work not only confirms the capability of OCT to temporal and spatial monitor of edema but is also able to locate focal conditions at some areas that might highly determine the prognosis and treatment decisions.

Keywords: Swept-source optical coherence tomography; ischemic stroke; cerebral edema; optical attenuation coefficient; middle cerebral artery occlusion.

‡Corresponding author.

1. Introduction

Stroke is a leading cause of death globally, accounting for enormous mortality and disability. While ischemia and subsequent cerebral infarction result in neurologic deficits, it is not the infarct itself that is responsible for most of the stroke deaths in the acute period. Instead, a majority of death and neurologic deterioration after infarction is closely related to the development of brain swelling. Greater volume of edema predicts poor outcome, independent of infarct volume and stroke severity. Cerebral edema is a leading cause of early death after ischemic stroke, which occurs in 10–78% of patients with ischemic stroke.[1] Although serious, cerebral edema has only limited medical and surgical treatment options available.[2] Considering the lack of effective treatment, early detection of cerebral edema with rapid intervention might improve clinical outcomes, including mortality and morbidity rate.

Current clinical imaging detection methods of edema include computerized tomography (CT) and Magnetic resonance imaging (MRI). On CT, edema manifests as decreased attenuation relative to surrounding normal parenchyma.[3] The early ischemic changes of cerebral edema on CT correspond to an increase in the intracellular and extracellular water components of affected brain tissue.[4,5] However, these changes are subtle, and CT is frequently normal in the first hours after stroke onset.[6,7] On MRI, edema produces high signal on T2-weighted imaging and low signal on T1-weighted imaging.[3] Nonetheless, the resolution of MRI determines that it is only capable of detecting edema long after stroke onset.[3]

Optical coherence tomography (OCT) is a non-invasive imaging technique with high resolution and speed. Optical attenuation coefficient (OAC) derived from OCT signals has been used to detect cerebral edema.[2,8–11] The swept-source OCT (SS-OCT) developed from basic OCT technique has improved imaging speed,[12] greater depth and range of structure visualization,[13,14] which allows for improvements in OCT-imaging in the clinic such as ophthalmology[15–17] and dermatology.[18] SS-OCT has also been successfully used to monitor edema formation and development in middle cerebral artery occlusion (MCAO) rats of the entire cortex.[19] When optimized depth-resolved estimation method was used, an *en face* OAC map was derived and applied to measure cerebral edema under the setting of ischemic edema in small animals *in vivo*.[2] Therefore, SS-OCT represents a promising tool for the detection of early edema after ischemic stroke.

Ischemic stroke is mainly caused by vessel occlusions which can be transient and permanent, and edema can be generated under both circumstances. There are several types of edema which are the results of different pathological processes.[3] Animal models are essential for the study of pathological mechanism, early diagnosis and therapeutic treatment of ischemic edema. A variety of ischemic stroke models in small animals have been developed and among them endothelin-1 (ET-1) and photochemical induced stroke models are less invasive and better mimic human stroke circumstances than the mechanical occlusion models (i.e., clips and sutures).[20–22] However, few studies have compared the characteristics of the edema generation and progression resulted from the two models, which can represent temporal and permanent ischemic strokes. The aim of the study is to use SS-OCT to monitor the edema derived from endothelin-1 and photochemistry and compare the measurements. The study could be potentially useful for revealing the edema characteristics induced by the two forms of strokes and might be useful for drug development studies to choose the suitable model to screen drugs.

2. Method

2.1. *Animal models*

All procedures were approved by the institutional Animal Care Committee of Northeastern University. All efforts were made to minimize animal suffering and to reduce the number of animals used. Sprague–Dawley male rats ∼ 3 months of age were used, with each weighing 250 g to 280 g. Animals were anesthetized by 3% sodium pentobarbital. Heart rate of the rats were monitored and kept at 500 beats per minute and temperature was maintained by a homoeothermic blanket system. The anesthetized rats were fixed on a stereotaxic apparatus (ST-5ND-C) with ear bars and a clamping device. After the fur was shaved, the skin was cut along the midline of the skull to expose the interparietal bone. The skull was grinded to the thickness of 0.1 mm to 0.2 mm in order to get clear OCT images.

For ET-1 induced model, the stereotaxic coordinates for injection of ET-1 or control (0.9% NaCl) were at 0.9 mm anterior, 5.2 mm lateral, and 8.7 mm

ventral relative to bregma. Three μl ET-1 (60 pmol/L in 0.9% NaCl) was injected at 1 μl/min and left another 3 min to allow fully absorption of the drug before needle was withdrawn.

For photochemically induced model, Rose Bengal (RB, Sigma-Aldrich, St Louis, MO, USA) was injected into the tail vein (20 mg/mL saline, 1 ml/kg bodyweight) and thrombosis was induced using parallel illumination (532 nm, the diameter of $\sim$ 2 mm, CNI Laser, MGL-III-532-5mW-1.5, Changchun, China) for 30 min. The animal was strictly shielded from light, minimizing diffuse Rose Bengal activation after laser illumination. The rat was then placed in the sample arm for data acquisition after treatment.

2.2. *OCT system and edema detection*

A wide FoV SS-OCT system with a central wavelength of 1310 nm and a spectral bandwidth of 100 nm providing an axial resolution of $\sim$ 7.5 μm in air was used as described previously.[2] The system operating at a 200 kHz swept rate and providing an axial resolution of $\sim$ 7.5 μm in air. The use of a 50-mm focal length objective lens makes the system to achieve the lateral resolution of $\sim$ 16 μm. Although the theoretical ranging depth of the system can reach $\sim$ 78 mm, we digitized each interference spectrum to 5000 points in this paper, which provided an actual measurement depth of $\sim$ 16 mm.

To calculate OAC from OCT signals, the influence of confocal characteristics was removed first through dividing by the axial point spread function proposed by Faber *et al.*,[23] an ODRE method was used as previously described.[24] This method can accurately calculate OAC at any depth. In brief, each pixel in OCT dataset was converted to the corresponding OAC value using Eq. (1), under the assumption that backscattered light reflected to the photodetector of the system was a fixed fraction of the attenuated light.

$$\mu[z] = \frac{I[z]}{2\Delta \sum_{i=z+1}^{N} I[i] + \frac{I[N]}{\mu[N]}}, \tag{1}$$

where $I[z]$ is the OCT signal of a pixel and $\mu[z]$ is the corresponding OAC, both of which are at depth z. Δ is the pixel size (relative to the axial resolution of the OCT system), and N is pixel numbers within a certain range of depth, $I[N]$ is the OCT signal of the last point N. To determine $\mu[N]$, the data taken from the end of the imaging depth was fitted to an exponential curve with model of $y = a \cdot \exp(-2\mu z) + b$. The resulting μ is the average attenuation coefficient of this data and is considered as the best approximation of $\mu[N]$, and b is the strength of the noise floor, which need to be subtracted from the original OCT signal before OAC calculation. After exponential fitting, the fitted μ was introduced into Eq. (1). A set of 3D OAC matrices are obtained after all the A-scan calculations finish.

En face OAC maps (edema maps) were reconstructed by averaging the OACs in the depth range of 0.7 mm to 1.5 mm below the surface of the cortex. Since the OAC value will decrease significantly as the water content of the brain tissue increases, the edema region will show a shadow. We separated this shadow region manually and count the number of pixels. The edema area is equal to the product of the area of a single pixel and the number of pixels.

2.3. *Data analysis*

Statistical analyses were conducted using GraphPad Prism (Graph-Pad Software Inc., San Diego, California). All experiments in the study were performed at least in triplicate (unless otherwise specified) from ≥ 3 independent experiments, and data are presented as mean $\pm$ standard error of the mean (SEM).

3. Results

3.1. *Edema images*

En face OAC images generated from averaging the OACs within the depth range from 0.7–1.5 mm were shown. In both models, shaded areas began to occur at earliest time point after baseline control, which was reflected by a decrease in OAC, indicating formation of cerebral edema.[2] Morphologically, in photochemically induced stroke model, the edema (shadow), is more focused and has clear boundary (Fig. 1), whereas edema induced by ET-1 is relatively diffuse, and the shape is more irregular (Fig. 2). Furthermore, the edema induced by irradiation sustained during the monitoring period (0–7 h) (Fig. 1), whereas the ET-1 induced edema was transient and faded with time (Fig. 2). Interestingly, although the majority part of edema is recovered at certain degrees, a small region (arrow) within the edema had no sign of recovery and went

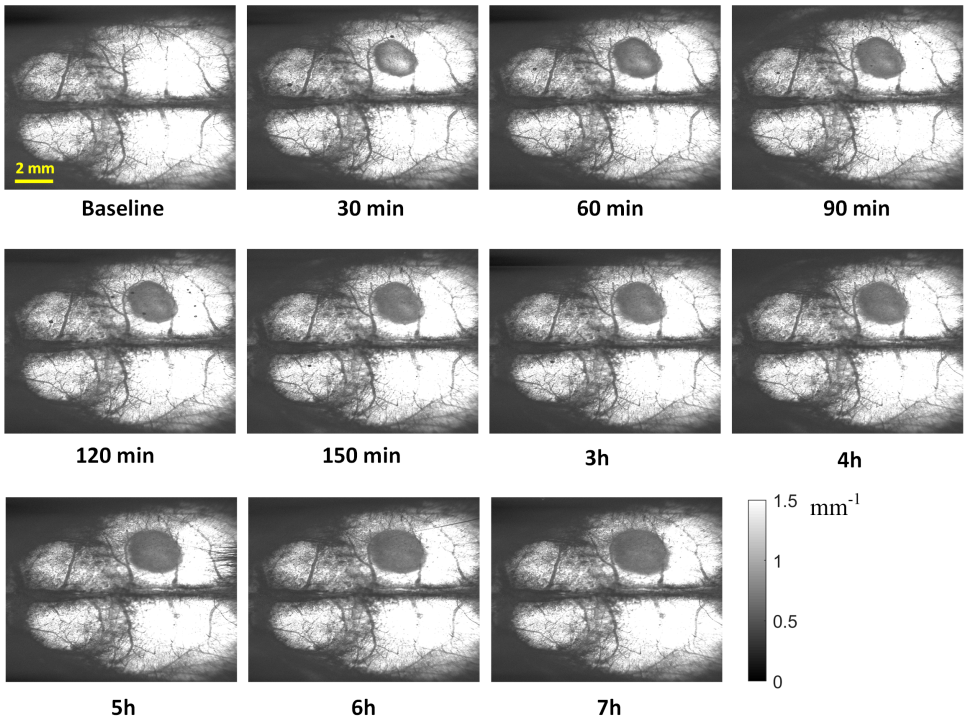

Fig. 1. En face OAC images after photochemical induction of thrombus. The shaded area indicates the formation of cerebral edema.

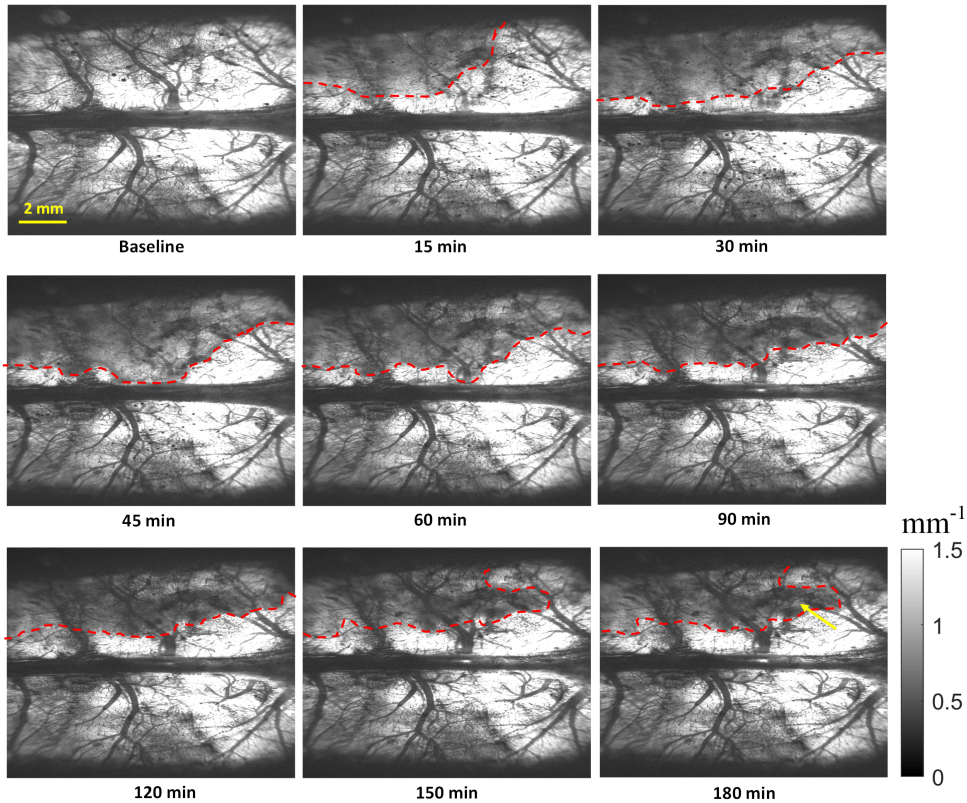

Fig. 2. En face OAC images taken after ET-1 injection. The shaded area indicates the formation of cerebral edema. The dotted line marked the boundary of the edema area at each time point, and the yellow arrow (in last picture) indicates the unrecovered region.

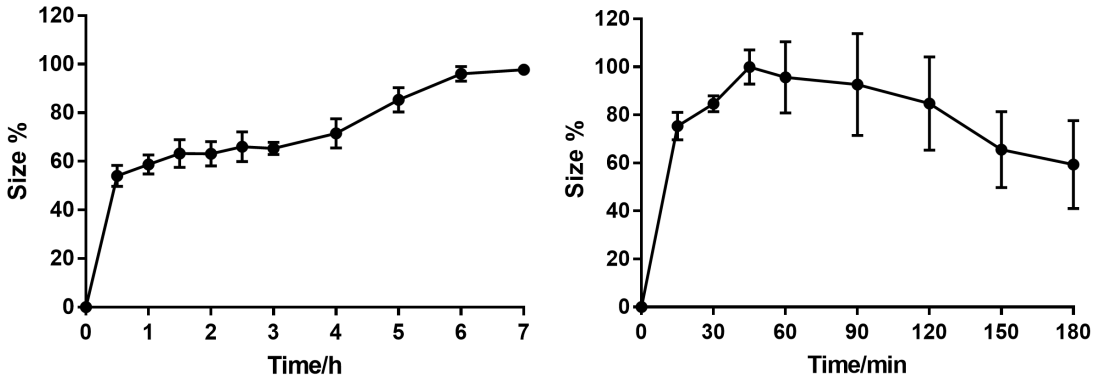

(a) (b)

Fig. 3. Edema sizes generated with time progression from two ischemic models in rats. Values were expressed as % means ± SEM ($n = 4$).

even worse, indicating by the OAC value reducing all the way until monitoring was terminated (Fig. 2).

3.2. *Edema sizes*

Edema sizes indicated by the sizes of the shade were measured from OAC data and are shown in Fig. 3. When focal ischemic stroke was induced photochemically, edema size progression was steady and reached the plateau at ∼ 6 h and sustained (Fig. 3 (a)). The lasting presence of edema is consistent with the permanent blockage of the blood flow during monitoring time window.

In contrast, ET-1 induced edema area peaks at ∼ 45 min after stimuli injection, and gradually decreased over time. At the last time point (180 min) of monitoring, the size of the edema reduced to ∼ 60% of the peak size (Fig. 3(b)). The effect of ET-1 on vessel constriction is transient and cerebral blood flow reperfusion occurs over several hours,[25,26] which may contribute to the gradual reduction of edema size observed after 45 min of ET-1 application (Fig. 3(b)).

3.3. *Edema indexes*

Edema indexes were reflected by the OAC signal intensities. We have previously reported that the severity of edema is reversely related to OAC value.[2,24] In this study, the OAC values at each time point in both models are shown in Fig. 4. When ischemia was induced photochemically, the average OAC value of the shaded area, which represents edema formation, decreased gradually with time where the slope became shallow after 3 h (Fig. 4(c)). Since the severity of edema was reversely related to OAC value, the edema index was represented by the percentage of OAC value decrease and plotted against each time points up to 7 h. As we can see in Fig. 4(e), edema was getting more condensed overtime until end of monitor. This is conceivable since the ischemia becomes more and more severe after blood vessel is blocked by the thrombus formed after irradiation. Comparatively, ET-1 induced condition was more complex. The shaded area progression was not uniform. In general, OAC value decreased rapidly until 30 min after vessel constrictor injection and gradually recovered thereafter (Fig. 4(d) red line). When edema index was considered, the value was increased quickly and then reduced (Fig. 4(f) red line), consistent with the blood flow reperfusion. Interestingly, although a major part of edema gradually recovered in ET-1 induced stroke rat brain, there is a small region (Fig. 3 arrow) with OAC value decreased all the way until the end of monitoring (Fig. 4(d) blue line), which indicates that edema index of this part is enhanced (Fig. 4(f) red line) despite of the general recovery of major part of the edema.

4. Discussion

Cerebral edema is one of the serious complications of ischemic stroke and accounts for the major causes of mortality after stroke onset. Nonetheless, once diagnosed, the treatment methods were limited. Therefore, early detection and evaluation of edema are essential. In this study, a transient and a permanent stroke models were used to induce edema of

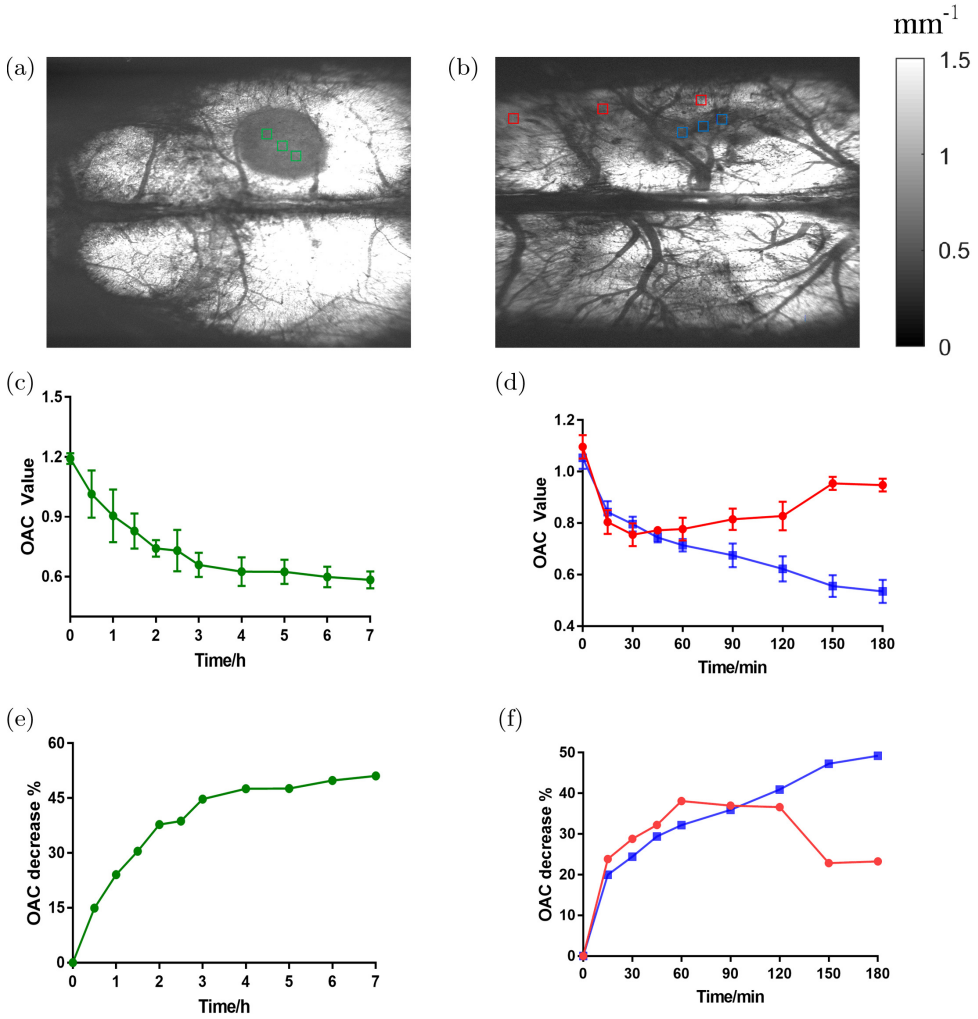

Fig. 4. Edema indexes generated with time progression from two ischemic models in rats. OAC values were calculated from three $240 \times 240\,\mu m^2$ regions as indicated in picture (a) and (b), using green, red and blue boxes, respectively. (c) and (d): Data were represented by OAC value over time (c): photochemical model, corresponding to green boxes in figure (a); (d): ET-1 model, corresponding to red and blue boxes in figure (b)) Values were expressed as means ± SEM ($n = 4$). E & F: Data were represented by the percentage of the OAC value decrease over time (e): photochemical model, corresponding to green boxes in Fig. (a); (f): ET-1 model, corresponding to red and blue boxes in figure (b)).

which characteristics were assessed and compared using SS-OCT technique.

The photochemical stroke model is established in 1985 by Watson *et al.*[27] by which cortical infarcts can be introduced in rats. Laser illumination is applied after a photosensitive dye is introduced into blood circulation. Peroxidative damage is caused by singlet oxygen generation at the site of endothelial cells on vessel wall. This leads to haemostasis process like vasoconstriction and platelet adhesion and aggregation, results in white thrombus formation and vessel occlusion, and thereby ultimately leads to distal territory ischemia. ET-1 works as a potent vasoconstrictor with long lasting effect. Stereotaxic injection of ET-1 induces a temporal ischemia in cerebral cortex. The blood flow reduction is rapid but not immediate[26] and reperfusion occurs over several hours.[28] This profile is more representative of human stroke than the immediate reduction and reperfusion seen with more traditional mechanical ischemic stroke model using intraluminal filament or clips, yet it is easier to handle and less invasive.[21]

OCT is a noninvasive real-time imaging technique that allows detecting of biological tissues with high resolution and high speeds.[29,30] OAC derived from OCT signals allows researchers to distinguish tissues under physiological and pathological status.[2,31] In this study, we focused on observing the

edema formation and progression in cerebral cortex based on OAC values, which was monitored real time by SS-OCT system. This system has greater spectral resolution[19] and higher penetration depth[32] than traditional spectral domain OCT. Cerebral edema can be generated shortly after ischemia is introduced, due to the greater water content within cerebral cells after extensive water penetration into the brain. The subsequent accumulation of acidic substances leads to cerebral cell membrane hyperpermeability within the affected cells.[10] The transmittance of infrared light increases with the water content of brain tissue, featured by the decrease of OAC value, and thereby, edema can be distinguished from normal tissue.[2,8]

Through monitoring with OCT, we found differences between the photochemical and ET-1 models. The edema formed by photochemically illumination had a steady increase in both size and index within the monitoring time (7 h). This is conceivable since the vessel after irradiation was completely blocked which generate permanent ischemia in cerebral tissue.[33] Interestingly, it was also noticed that at early stage of edema formation, i.e., at 30 min, the edema was merely detected as a ring shape, where the inner part has a lower degree of severity (higher OAC signal). The reason of this phenomenon is not clear, but one study has also observed the vasogenic edema as a shape of a "thin rim" in amyloid angiopathy.[3] As vasogenic edema was featured as the leakage of blood-brain barrier, it might indicate that the laser illumination-induced ischemia in our study has led to the blood-brain barrier hyperpermeability, which in turn caused the formation of a vasogenic edema from outside inwardly.

Comparatively, when ET-1, a vasoconstrictor, was used, blood vessels constricted to a certain degree that caused ischemia and generate edema, when the reperfusion occurred, most part of the edema recovered to some extent, nonetheless, there was a region where the damage to the cells was not recovered and even further deteriorated, indicated by OAC value kept decreasing. This is predictable as reperfusion injury is often observed clinically when a patient had blood reperfusion either after a transient ischemia stroke or after recanalization operations.[34] It was interesting to note that the edema underwent different pathophysiological processes after blood reperfusion. Although it is still debating whether reperfusion can augment or attenuate edema since conflicting results were obtained.[35–40] Our findings showed that blood reperfusion could have both effects on edema, presumably depending on the severity of the tissue damage during ischemia.

Intracranial pressure (ICP) and brain water content (BWC) are often used to estimate the degree of edema in brain, and these parameters only detect the global conditions of edema but would be much more difficult to apply to focal models of edema. Yet our results using SS-OCT showed that the optical properties can vary heterogeneously throughout the cerebral tissue relative to the site of injury. It is therefore speculated that focal detection of tissue conditions is essential to guide diagnosis and predict prognosis after stroke onset. This experiment provided preliminary evidence that reperfusion after reversible focal ischemia may trigger biological responses leading to the augmentation of cerebral damage established during ischemia (occlusion),[41] consistent with our finding that when certain tissue damage was caused that cannot be restored in transient stroke although the majority of edema was recovered at degrees.

It is noted that OAC reduction maybe caused by more than one factor. Studies have shown that cell necrosis also reduces OAC value.[42] We have compared with the T2-weighted and DWI sequence of MRI. The DWI signal in the shaded area changed significantly, but the T2-weighted signal had no obvious change. Therefore, it indicates that the shaded area is edema, not infarction. In addition, we also found that vessels surrounding the shaded area were compressed. Then, in mice undergo craniotomy, this phenomenon was not present. These observations are consistent with the pathological features of edema, suggesting the shaded area is edema area.

In summary, our study had utilized SS-OCT to noninvasively, spatially and temporally monitor cerebral edema development of two ischemic stroke models. Edema can be detected as early as 15 min after onset of stroke with high resolution. Photochemically induced permanent ischemic stroke leads to an edema with a gradual increase in both edema size and edema index. When transient ischemia was introduced with ET-1, the size and index of the edema increased rapidly and then decreased, consistent with blood reperfusion after short period of vessel constriction. It is noted that although major part of the edema is partially recovered, a certain

region of the brain tissue is not recovered by the end of monitoring, reflected by the persistent decrease of OAC value. This may indicate the development of cell membrane hyperpermeability, probably resulting in the permanent neuro cells damage. The results manifest that a global assessment of edema might not be applicable to represent the severity of the disease and the optical properties of focal conditions should be obtained and evaluated individually when treatment and prognosis are pursued. Our study highlights the potential of OCT for three-dimensional spatial monitoring of cerebral edema. The study extended the use of OCT to monitor the focal tissue conditions during edema progression with high resolutions.

Conflict of Interest

The authors declare that there are no conflict of interest related to this article.

Acknowledgments

This work was supported in part by National Natural Science Foundation of China (61771119 and 61901100), Hebei Provincial Natural Science Foundation of China (H2018501087 and H2019501010). Fundamental Research Funds for the Central Universities (N182304008).

References

1. R. Dhar, "Automated quantitative assessment of cerebral edema after ischemic stroke using CSF volumetrics," *Neurosci. Lett.* **724**, 134879 (2020).
2. J. Liu *et al.*, "Cerebral edema detection in vivo after middle cerebral artery occlusion using swept-source optical coherence tomography," *Neurophotonics* **6**(4), 045007 (2019).
3. M.-L. Ho, R. Rojas, R. L. Eisenberg, "Cerebral edema," *Am. J. Roentgenol.* **199**(3), W258–W273 (2012).
4. J. H. Garcia, "Experimental ischemic stroke: A review," *Stroke* **15**(1), 5–14 (1984).
5. E. Unger, J. Littlefield, M. Gado, "Water content and water structure in CT and MR signal changes: Possible influence in detection of early stroke," *Am. J. Neuroradiol.* **9**(4), 687–691 (1988).
6. C. Truwit *et al.*, "Loss of the insular ribbon: Another early CT sign of acute middle cerebral artery infarction," *Radiol.* **176**(3), 801–806 (1990).
7. P. Barber *et al.*, "Identification of major ischemic change: Diffusion-weighted imaging versus computed tomography," *Stroke* **30**(10), 2059–2065 (1999).
8. D. Liang *et al.*, "Cytotoxic edema: Mechanisms of pathological cell swelling," *Neurosurgical Focus* **22**(5), 1–9 (2007).
9. J. Liu *et al.*, "Simultaneous detection of cerebral blood perfusion and cerebral edema using swept-source optical coherence tomography," *J. Biophoton.* **13**(2), e201960087 (2019).
10. J. R. Thiagarajah, M. C. Papadopoulos, A. Verkman, "Noninvasive early detection of brain edema in mice by near-infrared light scattering," *J. Neurosci. Res.* **80**(2), 293–299 (2005).
11. C. L. Rodriguez *et al.*, "Decreased light attenuation in cerebral cortex during cerebral edema detected using optical coherence tomography," *Neurophoton.* **1**(2), 025004 (2014).
12. O. Carrasco-Zevallos *et al.*, "Live volumetric (4D) visualization and guidance of in vivo human ophthalmic surgery with intraoperative optical coherence tomography," *Sci. Rep.* **6**, 31689 (2016).
13. M. Adhi *et al.*, "Choroidal analysis in healthy eyes using swept-source optical coherence tomography compared to spectral domain optical coherence tomography," *Am. J. Ophthalmol.* **157**(6), 1272–1281. e1 (2014).
14. R. F. Spaide, H. Koizumi, M. C. Pozonni, "Enhanced depth imaging spectral-domain optical coherence tomography," *Am. J. Ophthalmol.* **146**(4), 496–500 (2008).
15. I. Grulkowski *et al.*, "High-precision, high-accuracy ultralong-range swept-source optical coherence tomography using vertical cavity surface emitting laser light source," *Opt. Lett.* **38**(5), (2013) 673–675.
16. I. Grulkowski *et al.*, "Retinal, anterior segment and full eye imaging using ultrahigh speed swept source OCT with vertical-cavity surface emitting lasers," *Biomed. Opt. Exp.* **3**(11), 2733–2751 (2012).
17. A.-H. Dhalla *et al.*, "Simultaneous swept source optical coherence tomography of the anterior segment and retina using coherence revival," *Opt. Lett.* **37**(11), 1883–1885 (2012).
18. W. J. Choi, R. K. Wang, "Volumetric cutaneous microangiography of human skin in vivo by VCSEL swept-source optical coherence tomography," *Quantum Electron.* **44**(8), 740 (2014).
19. J. Liu *et al.*, "Whole-brain microcirculation detection after ischemic stroke based on swept-source optical coherence tomography," *J. Biophoton.* **12**(10), e201900122 (2019).
20. J. Sharkey, "Perivascular microapplication of endothelin-1: A new model of focal cerebral ischaemia in the rat," *J. Cerebral Blood Flow Metabolism* **13**(5), 865–871 (1993).

21. V. Windle *et al.*, "An analysis of four different methods of producing focal cerebral ischemia with endothelin-1 in the rat," *Exp. Neurol.* **201**(2), 324–334 (2006).
22. O. W. Witte, Photochemical and endothelin models of focal brain ischemia, *Rodent Models of Stroke*, pp. 71–83, Springer (2010).
23. D. J. Faber *et al.*, "Quantitative measurement of attenuation coefficients of weakly scattering media using optical coherence tomography," *Opt. Exp.* **12**(19), 4353–4365 (2004).
24. J. Liu *et al.*, "Optimized depth-resolved estimation to measure optical attenuation coefficients from optical coherence tomography and its application in cerebral damage determination," *J. Biomed. Opt.* **24**(3), 1–11 (2019).
25. P. Dai *et al.*, "A pilot study on transient ischemic stroke induced with endothelin-1 in the rhesus monkeys," *Sci. Rep.* **7**, 45097 (2017).
26. I. M. Macrae *et al.*, "Endothelin-1-induced reductions in cerebral blood flow: Dose dependency, time course, and neuropathological consequences," *J. Cerebral Blood Flow Metabolism.* **13**(2), 276–284 (1993).
27. B. D. Watson *et al.*, "Induction of reproducible brain infarction by photochemically initiated thrombosis," *Ann. Neurology: Official J. Am. Neurol. Association Child Neurol. Soc.* **17**(5), 497–504 (1985).
28. J. Biernaskie *et al.*, "A serial MR study of cerebral blood flow changes and lesion development following endothelin-1-induced ischemia in rats," *Magn. Reson. Med., An Official J. Int. Soc. Magnetic Resonance Med.* **46**(4), 827–830 (2001).
29. U. Baran, Y. Li, R. K. Wang, "OCT-based in vivo tissue injury mapping," in *Optical Coherence Tomography and Coherence Domain Optical Methods in Biomedicine XX*, 2016, San Francisco, California, International Society for Optics and Photonics, p. 969725.
30. U. Baran *et al.*, "Automated segmentation and enhancement of optical coherence tomography-acquired images of rodent brain," *J. Neurosci. Methods* **270**, 132–137 (2016).
31. S. Yang *et al.*, "Correlation of optical attenuation coefficient estimated using optical coherence tomography with changes in astrocytes and neurons in a chronic photothrombosis stroke model," *Biomed. Opt. Exp.* **10**(12), 6258–6271 (2019).
32. J. Xu *et al.*, "Wide field and highly sensitive angiography based on optical coherence tomography with akinetic swept source," *Biomed. opt. Exp.* **8**(1), 420–435 (2017).
33. V. Labat-gest, S. Tomasi, "Photothrombotic ischemia: A minimally invasive and reproducible photochemical cortical lesion model for mouse stroke studies," *J. Vis. Exp. (76)*, e50370 (2013).
34. B. Piccardi *et al.*, "Reperfusion Injury after ischemic Stroke Study (RISKS): Single-centre (Florence, Italy), prospective observational protocol study," *BMJ Open* **8**(5), (2018).
35. W. T. Kimberly *et al.*, "Association of reperfusion with brain edema in patients with acute ischemic stroke: A secondary analysis of the MR CLEAN Trial," *JAMA Neurol.* **75**(4), 453–461 (2018).
36. G. Gartshore, J. Patterson, I. M. Macrae, "Influence of ischemia and reperfusion on the course of brain tissue swelling and blood–brain barrier permeability in a rodent model of transient focal cerebral ischemia," *Exp. Neurol.* **147**(2), 353–360 (1997).
37. D. R. Pillai *et al.*, "Cerebral ischemia–reperfusion injury in rats — A 3 T MRI study on biphasic blood–brain barrier opening and the dynamics of edema formation," *J. Cerebral Blood Flow Metabolism* **29**, 111846–1855 (2009).
38. B. Bell, L. Symon, N. M. Branston, "CBF and time thresholds for the formation of ischemic cerebral edema, and effect of reperfusion in baboons," *J. Neurosurgery* **62**(1), 31–41 (1985).
39. H. J. Irvine *et al.*, "Reperfusion after ischemic stroke is associated with reduced brain edema," *J. Cereb. Blood Flow Metab.* **38**(10), 1807–1817 (2018).
40. B. K. Cheripelli *et al.*, "Interaction of recanalization, intracerebral hemorrhage, and cerebral edema after intravenous thrombolysis," *Stroke* **47**(7), 1761–1767 (2016).
41. J. Aronowski, L. A. Labiche, "Perspectives on reperfusion-induced damage in rodent models of experimental focal ischemia and role of γ-protein kinase C," *ILAR J.* **44**(2), 105–109 (2003).
42. F. J. van der Meer *et al.*, "Apoptosis-and necrosis-induced changes in light attenuation measured by optical coherence tomography," *Lasers Med. Sci.* **25**(2), 259–267 (2010).